

Solvent Microextraction into a Single Drop

Michael A. Jeannot and Frederick F. Cantwell*

Department of Chemistry, University of Alberta, Edmonton, Alberta, Canada T6G 2G2

An analytical technique is described which combines solvent extraction with gas chromatographic (GC) analysis in a simple and inexpensive apparatus involving very little solvent consumption. A small drop (8 μ L) of a water-immiscible organic solvent, containing an internal standard, is located at the end of a Teflon rod which is immersed in a stirred aqueous sample solution. After the solution has been stirred for a prescribed period of time, the probe is withdrawn from the aqueous solution, and the organic phase is sampled with a microsyringe and injected into the GC for quantification. The observed rate of solvent extraction is in good agreement with a convective–diffusive kinetic model. Analytically, the relative standard deviation of the method is 1.7% for a 5.00-min extraction of the analyte 4-methylacetophenone into *n*-octane.

Conventional liquid–liquid extraction uses large amounts of solvent and is often tedious and time-consuming to perform. Techniques such as solvent extraction flow injection analysis,^{1–3} solid-phase extraction,^{4,5} and, more recently, solid-phase microextraction⁶ have been developed to overcome these disadvantages, and their use is becoming widespread. The present study is concerned with developing a complementary solvent microextraction technique using the principles of liquid–liquid extraction applied to very small volumes.

The solvent microextraction apparatus consists of a 1-mL vial which contains the aqueous sample and a rod-shaped Teflon probe hollowed out at one end and held in place by a washer and cap. The hollowed-out end of the Teflon probe is filled with 8 μ L of organic solvent (*n*-octane) and immersed in the aqueous sample. A magnetic stirrer is used to stir the aqueous phase. Although maximum sensitivity and precision are obtained by stirring until equilibrium is reached, it is generally more convenient to stir for a fixed, short time period (e.g., 5 min) at a constant stirring speed. After this time, the Teflon probe is removed from the aqueous sample, and a 1- μ L aliquot of the organic phase is taken by microsyringe and injected into a gas chromatograph (GC).

In addition to speed and convenience, there are some other advantages of this system. First, unlike in conventional extraction, neither phase is dispersed in the other, so no phase coalescence

is required after the extraction step. Second, the interfacial area is known with reasonable accuracy, facilitating the development of a theoretical model of mass transfer kinetics.

THEORY

Equilibrium Considerations. The limit of detection in the system is ultimately that of the GC detector. Thus, the concentration of analyte in the organic phase after stirring must be above this detection limit. The equilibrium concentration in the organic phase is given by

$$C_{o,eq} = \kappa C_{aq,eq} = \frac{\kappa C_{aq,initial}}{1 + \kappa V_o/V_{aq}} \quad (1)$$

where $C_{aq,initial}$ and $C_{aq,eq}$ are the initial and equilibrium aqueous-phase concentrations, V_o and V_{aq} are the organic- and aqueous-phase volumes, and κ is the distribution coefficient, defined by

$$\kappa = C_{o,eq}/C_{aq,eq} \quad (2)$$

Thus, κ and/or $C_{aq,initial}$ must be sufficiently large, and the phase ratio, V_o/V_{aq} , must be reasonably small to avoid detection problems. Also, in the interest of time, equilibrium may not be reached in an analytical application, so the organic phase concentration may be somewhat lower than $C_{o,eq}$.

Kinetic Considerations. The general rate equation for liquid–liquid extraction can be written as^{7–13}

$$\frac{dC_o}{dt} = \frac{A_i}{V_o} \bar{\beta}_o (\kappa C_{aq} - C_o) \quad (3)$$

where C_o is the concentration of analyte in the organic phase at time t , A_i is the interfacial area, $\bar{\beta}_o$ is the overall mass transfer coefficient with respect to the organic phase (in cm/s), and C_{aq} is the analyte concentration in the aqueous phase at time t .

- (1) Nord, L.; Bäckström, K.; Danielsson, L.-G.; Ingman, F.; Karlberg, B. *Anal. Chim. Acta* **1987**, *194*, 221–233.
- (2) Lucy, C. A.; Cantwell, F. F. *Anal. Chem.* **1989**, *61*, 101–107.
- (3) Lucy, C. A.; Yeung, K. K.-C. *Anal. Chem.* **1994**, *66*, 2220–2225.
- (4) Hagen, D. R.; Markell, C. G.; Schmitt, G.; Blevins, D. B. *Anal. Chim. Acta* **1990**, *236*, 157–164.
- (5) Kraut-Vass, A.; Thoma, J. J. *Chromatogr.* **1991**, *538*, 233–240.
- (6) Zhang, Z.; Yang, M. J.; Pawliszyn, J. *Anal. Chem.* **1994**, *66*, 844A–853A.

- (7) Danesi, P. R.; Chiarizia, R. *CRC Crit. Rev. Anal. Chem.* **1980**, *10*, 1–126.
- (8) Laddha, G. S.; Degaleesan, T. E. *Transport Phenomena in Liquid Extraction*; Tata McGraw-Hill: New Delhi, 1976; Chapter 3.
- (9) Tarasov, V. V.; Yagodin, G. A. In *Ion Exchange and Solvent Extraction*; Marinsky, J. A., Marcus, Y., Eds.; Marcel Dekker: New York, 1988; Chapter 4.
- (10) Davies, J. T.; Rideal, E. K. *Interfacial Phenomena*; Academic Press: New York, 1961; Chapter 7.
- (11) Pratt, H. R. C. In *Handbook of Solvent Extraction*; Lo, T. C.; Baird, M. H.; Hanson, C., Eds.; Wiley: New York, 1983; Chapter 3.
- (12) Hanna, G. J.; Noble, R. D. *Chem. Rev.* **1985**, *85*, 583–598.
- (13) Cussler, E. L. *Diffusion: Mass Transfer in Fluid Systems*; Cambridge University Press: Cambridge, UK, 1984; Chapters 1, 2, 9, 11.

Assuming rapid transfer across the liquid–liquid interface, the overall mass transfer coefficient can be expressed as

$$\frac{1}{\bar{\beta}_o} = \frac{1}{\beta_o} + \frac{\kappa}{\beta_{aq}} \quad (4)$$

where β_o and β_{aq} are the individual mass transfer coefficients for the organic and aqueous phases, respectively, defined by

$$\begin{aligned} \frac{1}{A_i} \frac{dn}{dt} &= \text{flux at interface} \\ &= \beta_{aq}(C_{aq} - C_{aq,i}) = \beta_o(C_{o,i} - C_o) \end{aligned} \quad (5)$$

The subscript *i* refers to concentrations immediately adjacent to the interface, while C_{aq} and C_o refer to bulk concentrations. It is assumed that equilibrium prevails at the interface at all times,^{8,13} so

$$C_{o,i}/C_{aq,i} = \kappa \quad (6)$$

Since C_{aq} can be written in terms of C_o from mass-balance considerations,

$$C_{aq} = \frac{C_{aq,initial}V_{aq} - C_oV_o}{V_{aq}} \quad (7)$$

eq 3 has the form of a reversible first-order reaction.

After substitution from eq 7, eq 3 is integrated to obtain the time dependence of the concentration in the organic phase:

$$C_o = C_{o,eq}(1 - e^{-kt}) \quad (8)$$

where k is the observed rate constant (s^{-1}),

$$k = \frac{A_i}{V_o} \bar{\beta}_o \left(\kappa \frac{V_o}{V_{aq}} + 1 \right) \quad (9)$$

Equations 4 and 9 reveal the influence of the experimental variables on analysis time. Thus, for rapid analysis, one must maximize A_i , β_o , and β_{aq} and minimize V_{aq} . The effects of V_o and κ on equilibration time depend on the magnitude of the capacity factor, $\kappa V_o/V_{aq}$, relative to 1.

Experimental values of C_o versus time can be fit to equation 8 to obtain both $C_{o,eq}$ and k , which yield both equilibrium (κ) and kinetic ($\bar{\beta}_o$) parameters. From eqs 2 and 7, at equilibrium, the distribution coefficient, κ , can be calculated:

$$\kappa = \frac{C_{o,eq}V_{aq}}{C_{aq,initial}V_{aq} - C_{o,eq}V_o} \quad (10)$$

The overall mass transfer coefficient can then be estimated by equation 9 since A_i can be estimated with reasonable accuracy.

Up to this point, the mass transfer coefficient has been treated as an empirical parameter relating the mass flux to the concentration difference, which serves as the driving force. For a particular combination of analyte and solvents, $\bar{\beta}_o$ will be a constant, provided that stirring rate and temperature are constant. The interpretation

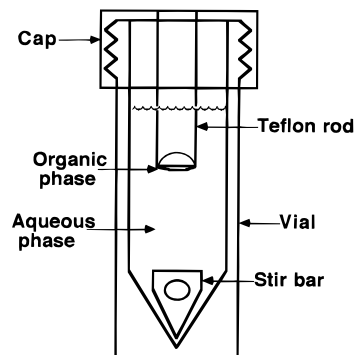


Figure 1. Side view illustration of the solvent microextraction system (approximately to scale). Magnetic stirrer not shown.

of the mass transfer coefficient entails modeling the system by, for example, Whitman two-film theory^{7,11,13} or Higbie's penetration theory.^{10,11,13} This will be discussed further in the Results and Discussion section.

EXPERIMENTAL SECTION

Chemicals. Caffeine (Aldrich, Milwaukee, WI), 4-methylacetophenone (Kodak, Rochester, NY), *n*-octane (BDH, Poole, England), *n*-dodecane (Aldrich), and toluene (BDH) were all reagent grade and used as received. Water was purified by the Nanopure system (Barnstead, Dubuque, IA).

Apparatus. The solvent microextraction apparatus is shown diagrammatically in Figure 1. The 1.0-mL minivial and stir bar were obtained from Alltech Associates (Deerfield, IL), stock no. 95010. The Teflon probe was fabricated in the Chemistry Department Machine Shop. A 1/8-in. drill bit with a rounded tip was used to machine out the hemispherical recess in one end of a 2.0-cm-long \times 0.40-cm-diameter Teflon rod, to contain the organic solvent. The speed of the stir bar was measured with a strobe lamp (Strobe 5K, Strobe Automation Ltd., England) and adjusted to the appropriate value. Temperature was maintained at 25 ± 0.02 °C by a circulating water bath (Lauda K-4/RD, Brinkmann, Rexdale, ON, Canada). A 10- μ L microsyringe (Model 701 N, Hamilton, Reno, NV) was used to introduce 8.0 μ L of organic phase into the probe and to sample and inject the organic phase into the GC after extraction. A Hewlett-Packard HP5840A gas chromatograph with packed column (Apiezon L stationary phase) and flame ionization detector (FID) was used for quantification. Helium was used as carrier gas at a flow rate of 20 mL/min, and column temperature was 200 °C.

For the determination of diffusion coefficients, the solvent was degassed with helium and pumped via a constant-pressure pump¹⁴ through 446 cm of loosely coiled (9-cm coil diameter) stainless steel tubing (0.02 in. i.d.), which was maintained at 25 ± 0.02 °C in a water bath (Lauda K-2). Sample plugs were injected via a six-port stainless steel injection valve (Valco HP series, Houston, TX) with a 10- μ L loop. The eluting peak was detected with a Varian UV-50 flow cell detector at 254 nm, and the peak was plotted on a strip chart recorder.

Extraction Studies. The model compound 4-methylacetophenone (4-MAP) was extracted from water into *n*-octane which contained 2.2 mM *n*-dodecane as internal standard. An aqueous 0.221 mM solution of 4-MAP was used in the kinetic studies, while several aqueous solutions of 4-MAP in the concentration range 0.109–0.543 mM were prepared for the analytical methodology studies.

(14) Fossey, L.; Cantwell, F. F. *Anal. Chem.* **1982**, *54*, 1693–1697.

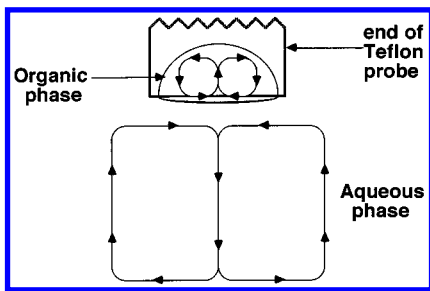


Figure 2. Enlarged view of the end of the Teflon probe showing the organic drop immersed in the aqueous phase. Fluid flow is illustrated conceptually with arrows (neglecting the rotational component for clarity), showing how circulation is induced in the organic phase.

After the solution was stirred for a known time, the probe was removed, and a $1\text{-}\mu\text{L}$ aliquot of the organic phase was taken with the microsyringe and injected into the GC for quantification. For the kinetic studies and isotherm measurement, the FID response was calibrated by injecting standard solutions of 4-MAP. This is not necessary, however, for routine analysis, as discussed later. In all cases, the fixed concentration of *n*-dodecane was present in the organic phase as an internal standard in order to correct both for evaporation of *n*-octane and for variable injection volumes. The analytical signal was taken as the peak area ratio of 4-MAP to *n*-dodecane.

Diffusion Coefficient Determinations. The determination of diffusion coefficients was based on the Taylor dispersion method.^{15–19} The observed peaks were nearly symmetrical, with an asymmetry factor of about 1.1 at 10% of peak height. Therefore, peak width was measured by the “tangent” method.¹⁷ The calculations require an accurate calibration of the tubing radius. This was done by injecting compounds having known diffusion coefficients. Caffeine in water, with $D = (6.3 \pm 0.4) \times 10^{-6} \text{ cm}^2/\text{s}$,²⁰ and toluene in *n*-octane, with $D = (2.99 \pm 0.06) \times 10^{-5} \text{ cm}^2/\text{s}$,²¹ were employed. Both yielded similar results, with an average radius and standard deviation of $0.0279 \pm 0.0005 \text{ cm}$.

RESULTS AND DISCUSSION

Diffusion Coefficients. The treatment of observed extraction rates with theoretical convective–diffusive mass transfer models requires a knowledge of the diffusion coefficients of 4-MAP. These were measured by the Taylor dispersion method to be $D_{\text{aq}} = (7.0 \pm 0.2) \times 10^{-6} \text{ cm}^2/\text{s}$ in water and $D_{\text{o}} = (2.3 \pm 0.05) \times 10^{-5} \text{ cm}^2/\text{s}$ in *n*-octane, at 25°C , based on three replicate measurements. However, measurement of diffusion coefficients is not necessary in an analytical application where simple calibration suffices.

Flow Pattern. In the apparatus shown in Figure 1, the aqueous phase is well stirred. The flow patterns in both the aqueous and organic phases were made visible to the eye by

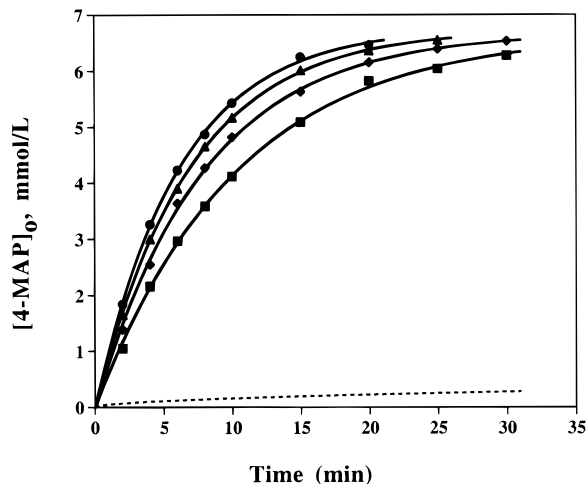


Figure 3. Plots of concentration of 4-methylacetophenone in *n*-octane versus stirring time at various aqueous phase stirring rates. Points indicate experimental data: (■) 900, (◆) 1200, (▲) 1500, and (●) 1800 rpm. Solid lines represent the fit of eq 8 with the parameters $C_{\text{o,eq}}$ and k given in Table 1. Dashed line represents extraction profile for the case of no stirring as predicted by semiinfinite diffusion.¹⁰

suspending charcoal powder in each phase while stirring only the aqueous phase. The circulatory flow in each phase consists of both a horizontal–rotational component and a vertical–toroidal component. The toroidal flow in each of the phases is shown diagrammatically in Figure 2. The origin of such flow in the stirred aqueous phase is obvious. The reason for it in the organic phase is as follows: As the aqueous phase sweeps radially inward in a horizontal plane past the aqueous–organic interface, the frictional drag on the organic layer induces a parallel motion in the organic phase. When the flow streamlines in each phase converge at the central axis of the vial, they change direction and move vertically into their respective bulk phases. The situation is analogous to that which prevails in a liquid drop that is falling or rising through an immiscible liquid.^{7,22} Circulation in the organic phase will affect the rate of solvent extraction only if $1/\beta_{\text{o}}$ is not much smaller than κ/β_{aq} (eq 4); however, in any event, this circulation has the desirable effect of homogenizing the organic phase prior to gas chromatographic analysis.

Kinetics. Shown as data points in Figure 3 are plots of concentration vs time for extraction of 4-MAP from 1.00 mL of a $2.21 \times 10^{-4} \text{ mol/L}$, stirred aqueous solution into an $8.0\text{-}\mu\text{L}$ droplet of *n*-octane. Four different stirring rates between 9.0×10^2 and $1.80 \times 10^3 \text{ rpm}$ were employed. Slower stirring rates could not be measured with the strobe lamp, and faster stirring rates resulted in dislodgement of the organic droplet from the rod. The solid lines through the four sets of data points represent the fitting of eq 8 to the data using a nonlinear least-squares program in the software package KaleidaGraph.²³ Values of the fitting parameters $C_{\text{o,eq}}$ and k are presented in columns 2 and 3 of Table 1. Within experimental error, the equilibrium concentration $C_{\text{o,eq}}$ is independent of stirring rate, so κ , from eq 10, is also a constant, independent of stirring rate (column 4 in Table 1). Evidently, the rate constant k is constant at a fixed stirring rate, so $\bar{\beta}_{\text{o}}$, from eq 9, is also constant (column 5 in Table 1). However, at higher stirring rates, k and $\bar{\beta}_{\text{o}}$ increase.

(15) Grushka, E.; Kikta, E. J., Jr. *J. Phys. Chem.* **1974**, *78*, 2297–2301.

(16) Grushka, E.; Maynard, V. R. *J. Phys. Chem.* **1973**, *77*, 1437–1442.

(17) Ouano, A. C. *Ind. Eng. Chem. Fundam.* **1972**, *11*, 268–271.

(18) Pratt, K. C.; Slater, D. H.; Wakeham, W. A. *Chem. Eng. Sci.* **1973**, *28*, 1901–1903.

(19) Levenspiel, O.; Smith, W. K. *Chem. Eng. Sci.* **1957**, *6*, 227–233.

(20) Liley, P. E.; Reid, R. C.; Buck, E. In *Chemical Engineers' Handbook*, 6th ed.; Perry, R. H., Green, D. W., Eds.; McGraw-Hill: New York, 1984; Chapter 3, pp 258–259.

(21) Chang, P.; Wilke, C. R. *J. Phys. Chem.* **1955**, *59*, 592–596.

(22) Laddha, G. S.; Degaleesan, T. E. *Transport Phenomena in Liquid Extraction*; Tata McGraw-Hill: New Delhi, 1976; Chapters 6, 7.

(23) KaleidaGraph 3.0, Synergy Software, Reading, PA.

Table 1. Equilibrium and Kinetic Parameters for Extraction of 4-MAP from Water into 8.0 μL of *n*-Octane at Four Stirring Rates, Plus Diffusion Film Thickness in the Water Phase

stirring rate (rpm)	$C_{0,\text{eq}}$ (mol/L) $\times 10^3$	k (s^{-1}) $\times 10^3$	κ (L/L)	$\bar{\beta}_0^a$ (cm/s) $\times 10^4$	$t_{1/2}^b$ (min)	δ_{aq} (μm)
900	6.67 ± 0.07	1.61 ± 0.04	39.8 ± 0.6	1.24 ± 0.04	7.2	14.3
1200	6.69 ± 0.05	2.10 ± 0.05	39.9 ± 0.4	1.61 ± 0.04	5.5	11.0
1500	6.74 ± 0.03	2.42 ± 0.03	40.3 ± 0.2	1.85 ± 0.03	4.8	9.4
1800	6.77 ± 0.05	2.70 ± 0.05	40.6 ± 0.4	2.06 ± 0.04	4.3	8.4

^a $\bar{\beta}_0$ is from eq 9 with $A_i = 0.079 \text{ cm}^2$, $V_{\text{aq}} = 1.00 \times 10^{-3} \text{ L}$, and $V_o = 8.00 \times 10^{-6} \text{ L}$. ^b Half-time calculated as $t_{1/2} = \ln 2/k$.

It has often been observed for solvent extraction systems that $\bar{\beta}_0$ is related to stirring rate S by an expression of the form⁷

$$\log \bar{\beta}_0 = \log M + p \log S \quad (11)$$

For the data in Table 1, a plot of $\log \bar{\beta}_0$ vs $\log S$ is linear with a slope of 0.74 ± 0.06 , an intercept of -6.1 ± 0.2 , and a correlation coefficient $R^2 = 0.988$. The value of $p = 0.74$ is intermediate between the value of 1.0 that is often observed for the "Lewis cell", in which two immiscible liquids are stirred independently without disturbing the interface,^{7,24} and the value of 0.5 predicted by the Levich equation for a rotating disk and observed in the Albery rotated extractor.²⁵

The absolute values of $\bar{\beta}_0$ obtained in the microextraction system are somewhat larger than those observed in the Lewis cell²⁴ and in the so-called "rapid-stir cell",^{26,27} in which droplets of one phase are dispersed in the other phase. This is because Lewis cells are stirred more slowly to avoid disturbing the interface, while in rapid-stir cells the shearing forces between the droplets and the continuous phase are limited because the dispersed droplets tend to move along with the continuous phase. Although $\bar{\beta}_0$ in the microextraction system is relatively large, the small A_i/V_o ratio (eq 3) limits the rate of extraction compared to the rapid-stir cell.

The absolute values of $\bar{\beta}_0$ obtained in the microextraction system, while larger than those for stirred systems, are comparable to those observed for falling and rising drops.²² For example, at a stirring rate of 1500 rpm, the rotational velocity of water in the vicinity of the probe tip was measured to be 12 cm/s by observing the movement of a single charcoal particle with the aid of a strobe lamp. For a drop of *n*-octane rising through water with a terminal velocity, U_t , of 12 cm/s, theory predicts mass transfer coefficients of $\beta_{\text{aq}} = 8 \times 10^{-3} \text{ cm/s}$ and $\beta_o = 16 \times 10^{-3} \text{ cm/s}$. From eq 4, taking $\kappa = 40 \text{ L/L}$ for 4-MAP, $\bar{\beta}_0$ for the rising drop system would therefore be $2 \times 10^{-4} \text{ cm/s}$. This is essentially the same as the value $1.9 \times 10^{-4} \text{ cm/s}$ reported in Table 1 at the appropriate 1500 rpm stirring rate.

The dashed line in Figure 3, shown for comparison, is the concentration vs time profile predicted for the case in which there is no stirring. This rate curve is based on a semiinfinite linear diffusion model.¹⁰ After 30 min, the extent of extraction in such a stagnant system would be only about 4% of the equilibrium value. Clearly, stirring produces a dramatic increase in the extraction rate compared to the stagnant case.

Mass Transfer Model. To gain some insight into the nature of the extraction process, the mass transfer coefficient $\bar{\beta}_0$ may be interpreted in terms of a convective-diffusive mass transfer model. The popular Whitman two-film theory,^{7,11,13} is employed.

Film theory postulates steady-state diffusion (after a short lag time) across stagnant solvent layers of thickness δ_o and δ_{aq} adjacent to the interface in the organic and aqueous phases, respectively. In either the organic or the aqueous phase, the mass transfer coefficient $\beta = D/\delta$, where D is the diffusion coefficient of the solute and δ is the film thickness in the appropriate phase. Thus, according to film theory, eq 4 can be written as

$$\frac{1}{\bar{\beta}_0} = \frac{\delta_o}{D_o} + \frac{\kappa \delta_{\text{aq}}}{D_{\text{aq}}} \quad (12)$$

If the two terms on the right-hand side of eq 12 are comparable in magnitude, then simultaneous evaluation of both film thicknesses is not possible from studies of only one solute (i.e., only one κ). However, in the present case, κ is large, so the first term on the right in eqs 4 and 12 can be neglected, and resistance to mass transfer in the aqueous phase is the rate-determining step for extraction. With this approximation, δ_{aq} can be evaluated since D_{aq} is independently known. Calculated values are presented in the seventh column of Table 1.

Analytical Methodology. The equilibrium distribution isotherm was measured by the solvent microextraction technique using five aqueous solution concentrations of 4-MAP in the range 0.109–0.543 mM. The aqueous phase was stirred at 1800 rpm for 30 min, by which time the extraction was about 99% of the way to equilibrium. The isotherm is linear in this concentration range, with a slope of $\kappa = 38.5 \pm 1.7 \text{ L/L}$, an intercept of zero ($0.06 \pm 0.46 \text{ mmol/L}$), and a correlation coefficient (R^2) of 0.994. Equilibrium organic-phase concentrations were measured by GC, and equilibrium aqueous-phase concentrations were calculated with eq 7. At equilibrium, about 24% of the initial aqueous-phase concentration has been extracted into the organic phase.

In an analysis, it is desired to evaluate $C_{\text{aq,initial}}$ for an aqueous sample solution based upon the measured value of C_o at some stirring time, t . Combining eqs 1 and 8 gives the expression

$$C_{\text{aq,initial}} = C_o \left[\frac{1 + \kappa V_o/V_{\text{aq}}}{\kappa(1 - e^{-kt})} \right] \quad (13)$$

The bracketed term will be a constant which can be evaluated by extracting a standard solution of known $C_{\text{aq,initial}}$, provided that the concentrations are in the linear region of the distribution isotherm for both sample and standard, and provided that the following are the same for both sample and standard: V_o/V_{aq} , k (i.e., same

(24) Higuchi, T.; Michaelis, A. F. *Anal. Chem.* **1968**, *40*, 1925–1931.

(25) Albery, W. J.; Burke, J. F.; Leffler, E. B.; Hadgraft, J. J. *Chem. Soc., Faraday Trans.* **1976**, *72*, 1618–1626.

(26) Amankwa, L.; Cantwell, F. F. *Anal. Chem.* **1989**, *61*, 1036–1040.

(27) Cantwell, F. F.; Freiser, H. *Anal. Chem.* **1988**, *60*, 226–230.

stirring rate), and stirring time, t . Equation 13 shows that it is not necessary to stir until equilibrium is reached, provided that the stirring conditions and time are reproduced, though, of course, the closer the system is brought to equilibrium, the less critical are the stirring conditions and time.

From eq 13, it may be inferred that, since the GC signal (employing internal standard) is proportional to C_0 , then a plot of GC signal vs $C_{\text{aq,initial}}$ for a series of standard concentrations should yield a linear calibration curve. The same five aqueous 4-MAP solutions which were employed in measuring the distribution isotherm were each subjected to 5.00 min of stirring in the microextraction apparatus, and the measured GC signals were plotted vs initial aqueous concentration of 4-MAP. This calibration curve was linear, with a slope of 4.88 ± 0.13 L/mmol, an intercept of zero (-0.001 ± 0.05), and a correlation coefficient (R^2) of 0.998. After 5 min of stirring, the extraction is only slightly more than half way to equilibrium, and yet good precision is obtained for the calibration curve. The precision was further tested by performing 5-min extractions and GC analysis on 10 replicate, 1.00-mL aliquots of the aqueous solution of $C_{\text{aq,initial}} = 1.77 \times 10^{-4}$ mol/L. The relative standard deviation was 1.7%, which is quite acceptable for a solvent extraction GC method.

In cases where the aqueous sample is plentiful, it would be possible to expose the organic drop to a flowing stream of sample rather than to a stirred, fixed volume of sample. An advantage of the flowing aqueous sample is that the organic drop continuously would be in contact with fresh aqueous sample having the initial analyte concentration. Such a situation is equivalent to setting V_{aq} equal to infinity in eqs 1, 7, 9, 10, and 13, and as a consequence, the organic-phase analyte concentration would be approaching an equilibrium value of $\kappa C_{\text{aq,initial}}$. The fluid dynamic effect of linear flow on the mass transfer coefficient would have to be characterized.

Comparison of the proposed solvent microextraction technique with the technique of solid-phase microextraction (SPME) into a polymer film coated on a fused silica fiber⁶ reveals that the two techniques are comparable in terms of precision, sensitivity, and analysis time. SPME has the advantage that there is no solvent peak in the GC. However, this advantage is offset by the cost of a more elaborate and expensive apparatus than is employed in solvent microextraction and by the fact that analyte desorption from the polymer in the GC injector is slower than conventional solvent evaporation and leads to analyte peaks showing greater tailing. Recent modifications of SPME accelerate the desorption rate but at the cost of an even more complex SPME injection system,²⁸ while recent experiments in this laboratory demonstrate that solvent microextraction can be performed very successfully with the simplest of devices, a 1- μ L droplet suspended in the aqueous solution from the tip of a conventional microsyringe.²⁹ Automation of this microsyringe system with a conventional autosampler is an obvious possibility. Such automation has been demonstrated for SPME.³⁰

A second advantage of the SPME system is its ready adaptability to "head-space" analysis. No attempt has yet been made to adapt the solvent microextraction system to head-space analysis, though recently a liquid droplet has been reported for sampling of gas streams.³¹⁻³³

Current and future experiments in this laboratory involve the use of the 1- μ L droplet device and are directed at two goals: first, the relative merits of film and penetration theories are being investigated, and second, solvent microextraction is being applied to "real-world" samples.

ACKNOWLEDGMENT

Dr. J. W. Lown kindly allowed the use of his HP5840A gas chromatograph for these studies. This work was supported by the Natural Sciences and Engineering Research Council (NSERC), and M.J. was further supported by an NSERC Studentship.

Received for review January 16, 1996. Accepted April 1, 1996.[®]

AC960042Z

[®] Abstract published in *Advance ACS Abstracts*, May 15, 1996.

(28) Górecki, T.; Pawliszyn, J. *Anal. Chem.* **1995**, *67*, 3265-3274.

(29) Jeannot, M.; Cantwell, F. F. Unpublished results.

(30) Arthur, C. L.; Killam, L. M.; Buchholz, K. D.; Pawliszyn, J. *Anal. Chem.* **1992**, *64*, 1960-1966.

(31) Liu, S.; Dasgupta, P. K. *Anal. Chem.* **1995**, *67*, 2042-2049.

(32) Cardoso, A. A.; Dasgupta, P. K. *Anal. Chem.* **1995**, *67*, 2562-2566.

(33) Liu, H.; Dasgupta, P. K. *Anal. Chem.* **1995**, *67*, 4221-4228.